



PHYSICOCHEMICAL PROPERTIES OF BRAZILIAN BIOMASSES: POTENTIAL APPLICATIONS AS RENEWABLE ENERGY SOURCE

Glauber Cruz

University of São Paulo, Engineering School of São Carlos, Mechanical Engineering Department, São Paulo, Brazil
glauber.cruz@usp.br

Carlos E. M. Braz

State University Paulista “Júlio de Mesquita Filho”, Chemistry Institute of Araraquara, São Paulo, Brazil
carloosedumb@iq.unesp.br

Sérgio Lucas Ferreira

University of São Paulo, Engineering School of São Carlos, Mechanical Engineering Department, São Paulo, Brazil
serggiolf@yahoo.com.br

Antonio Moreira dos Santos

University of São Paulo, Engineering School of São Carlos, Mechanical Engineering Department, São Paulo, Brazil
asantos@sc.usp.br

Paula Manoel Crnkovic

State University Paulista “Júlio de Mesquita Filho”, Chemistry Institute of Araraquara, São Paulo, Brazil
paulam@sc.usp.br

Abstract. Biomass is a promising renewable energy source and its properties often form the basis for the chosen thermal process. Brazil has developed advanced programs for the implementation of different types of biomasses for energy purpose. Fundamental knowledge on thermal behavior of energy sources is still scarce and there is no sufficient information for oxidative atmosphere, being these essential to the development and optimization of technological processes. This study provides physicochemical properties of three biomass samples in natura: coffee husk, rice husk, and tucumã seed. Experiments were performed in a thermogravimetric analyzer (TGA/DTG and DTA) under different atmospheres: combustion (synthetic air), pyrolysis (pure nitrogen) and oxy-combustion with two different ratios of CO₂/O₂ (60/40% and 80/20%). Different techniques, such as ultimate analysis, calorimetry, SEM micrographs, X-ray diffraction, Raman and FTIR spectroscopy and Contact angle were also used to characterize the samples. The samples by TG curves presented three decomposition stages in air and CO₂/O₂ and two stages in nitrogen atmospheres. X-rays diffractograms showed crystallinity indexes of 64.3, 57.5 and 57.4% for rice husk, coffee husk and tucumã seed, respectively. Morphology of the samples revealed different structures (external epidermis, disorder and spongy structure). The calorific values found are within the range of 15 up to 21 MJ kg⁻¹. Raman and FTIR spectroscopy evaluated mainly the presence of oxygen, carbon and hydrogen containing functional groups and both crystalline and amorphous constructions confirmed by X-ray. Wettability showed that rice and coffee husks had a superhydrophilic character, whereas tucumã seeds had a superhydrophobic character. Tucumã seed is the strongest candidate to be used as a bioenergy source due to its high heat value, moisture and ash content low, high carbon content and superhydrophobicity.

Keywords: biomass characterization, combustion and oxy-fuel combustion, thermal analysis, wettability

1. INTRODUCTION

The vegetation of countries, such as Brazil, Spain, Africa, China and India, has shown a great variety of lignocellulosic materials (biomasses), that can to be used as an important source of feedstock for the production of bioenergy or biofuels (Sasmal *et al.*, 2012; García *et al.*, 2010; Guimarães *et al.*, 2009; Ramajo-Escalera *et al.*, 2006).

Brazil is a pioneer country in the production of renewable fuels (Lira *et al.*, 2013) and is also among the largest producers and consumers of rice worldwide (Guimarães *et al.*, 2009; Tsai *et al.*, 2006). Lira *et al.* (2013) reported that the utilization of tucumã seeds to produce bio-oil has shown a positive effect on the production of electricity in isolated communities in the Amazon State in Brazil.

The combustion process of biomasses comprises the burnout in an ambient rich in oxygen or air. In this process are taken into account the types and fuel properties, process conditions, particles size, air flow rate and fuel moisture affecting the combustion characteristics as well as generation and transfer heat, and the reaction rates. A key parameter in the combustion process of solid fuels is the primary air flow rate, which evaluates the quantity of oxygen and heat transfer by convection (Zhao *et al.*, 2008; Senneca, 2007). According to Aghamohammadi *et al.* (2011) and Han & Jin (2008), the biomass combustion involves a series of successive exothermic chemical reactions between the fuel and

oxidizing for production of energy and heat. The thermal degradation of biomass is a very complex process of interdependent reactions due to the existence of several different monomers, oligomers and polymers in the fuels composition (Leroy *et al.*, 2006).

Babu (2008) investigated a process called pyrolysis, in which a lignocellulosic material suffers a thermal degradation in the absence of air or oxygen to produce solids (coal, biochar or biocoal), liquids (tar and other organics) and gaseous products. This process breaks off the solid matrix into low molecular mass gases (volatiles) and carbonaceous char (Leroy *et al.*, 2006). The process is not an independent method, but a first step to the gasification or combustion process. For this reason, the process of biomass pyrolysis has gained relevance (Van der Stelt *et al.*, 2011; Tsai *et al.*, 2006).

A high concentration emitted of CO₂ during the process of burning of conventional fossil fuel, is the main problem in the power plants for refinement of these products. An alternative is the oxy-fuel combustion process, which is a technology applied to capture CO₂ and other gases that cause the greenhouse effect during the combustion of coal, biomass or blends. This process releases a mixture with oxygen (free air) and recycled flue gas, which mainly contains CO₂ e H₂O ready to be captured (Álvarez *et al.*, 2011; Riaza *et al.*, 2011; Arias *et al.*, 2008).

The characterization of biomasses is possible to obtain a perfect knowledge of their properties, which allows a good definition for its choice and use as new energy sources (Ramajo-Escalera *et al.*, 2006). This study evaluates the thermal degradation process of three biomasses *in natura*: coffee husks, rice husks and *tucumã* seed using inert (N₂), oxidizing (synthetic air) and oxy-combustion (60/80% CO₂ and 40/20% O₂) atmospheres. Experiments were performed on a Thermogravimetric balance (TG/DTG) and in a Differential Thermal Analyzer (DTA). Other analytical techniques for the evaluation of morphological aspects (Scanning Electron Microscopy - SEM) and structural (X-Ray Diffraction, Fourier Transform Infrared Spectroscopy - FTIR, Raman Scattering Spectroscopy, and Wettability or Angle Contact - AC) were also used to identify the biomass potentials as new sources for the production of bioenergy or biofuels.

2. MATERIAL AND METHODS

2.1 Origin of Biomasses

Three biomass samples *in natura*: coffee husks (São Paulo State – Southeast region), rice husks (Maranhão State – Northeast region) and *tucumã* seeds (Pará State – North region) were selected for this study. An interesting point is that the vegetation and climate characteristics of each region are well defined and differentiated, facilitating the plantation of several native species, conditions requiring specific of cultures.

2.2 Preparation of Samples

The samples were received *in natura* and underwent pretreatments that consisted in washing with running water to remove impurities, grinding in laboratory knives mill to decrease the particles size and subsequent sieving for the separation in the required granulometric range. For all the samples the particles average sizes were 0.46 mm.

2.3 Thermal Analysis (TG/DTG and DTA) and Elemental Analysis (EA)

The elemental chemical composition was obtained in EA1110-CHNS-O CE Instruments equipment (Elemental Analyzer). Also include was the moisture and ashes content, as shown in Tab. 1. The moisture and ash content were determined termogravimetrically under controlled temperature by TG curves in oxidizing atmosphere (synthetic air).

The High Heating Value (HHV) was measured in an adiabatic oxygen IKA C 2000 calorimeter bomb (Tab. 1).

The TG/DTG and DTA non-isothermal experiments were performed in Shimadzu analyzers, TGA-50H and DTA-51 models, respectively. The oxidizing (synthetic air), inert (pure nitrogen), and two oxy-fuel combustion concentrations (60/80% CO₂ and 40/20% O₂) atmospheres, were promoted by the carrier gas with a dynamic flow rate of 100 mL min⁻¹. For these experiments was used constant heating rate utilized of 10 °C min⁻¹ from room temperature up to 700 °C. The samples mass were (10.0 ± 0.5) mg and alumina crucible. The tests were performed in duplicate and the average values and standard deviations were considered and showed in Tab. 2.

2.4 X-Ray Diffraction (X-Ray)

X-Ray diffractograms were obtained using a D 5000 X-Ray Diffractometer Siemens brand. The operating conditions were 40 kV, 20 mA, radiation of CuK_α of $\lambda = 1.541 \text{ \AA}$ and angle of 2θ with scanning between 4 and 80 °, under time step of 0.020 s⁻¹.

2.5 Fourier Transform Infrared Spectroscopy (FTIR)

A Perkin Elmer brand Spectrum 200 spectrophotometer (IR-TF) from 4000 to 400 cm^{-1} range, by Fourier Transformed and KBr (Potassium Bromide) pellets was used to obtain the absorption spectra in infrared region for the biomasses *in natura*.

2.6 Scanning Electronic Microscopy (SEM images)

The morphological analysis of the biomass samples *in natura* was performed in LEO 440 Scanning Electron Microscope equipment of 1,000 times amplitude and analyzed by SEM images produced.

2.7 Raman Scattering Spectroscopy (Raman spectra)

The Raman spectra for the biomasses *in natura* were obtained by 2000 Renishaw Microscope System Micro-Raman Scattering Spectroscopy using 514.5 nm lines of argon ion laser in the range from 800 to 1800 cm^{-1} (first order spectra), com 1 accumulated of 30s. The spectra were fitted after baseline subtraction using one Gaussian curve at 1332 cm^{-1} (used displacement of the natural diamond for calibration), which is demonstrated for the suitable curve shape (Azevedo *et al.*, 2009).

2.8 Wettability or Contact Angle (CA)

Wettability measurements were obtained using an Easy Drop System - DO 4010 Goniometer with computational program - DSA - Drop Shape Analysis, from Krüss German brand, at room temperature and controlled atmospheric pressure. A drop volume of 5 μL with deionized water was deposited onto the substrates by Sessile Drop Fitting method (Young-Laplace equation). The images were duplicated and captured the first measure with accuracy $\pm 3^\circ$, immediately after the drop placement on the surface to avoid the perturbation by evaporation process (Azevedo *et al.*, 2009; Krüss, 2005).

3. RESULTS AND DISCUSSIONS

3.1 Thermal and Elemental Analysis

Table 1 shows details of the physical and chemical properties of the biomasses for biofuel production. The elemental analysis, moisture and ash content of the samples are showed in Tab. 1. The results revealed that the oxygen content in rice husks was higher than that of coffee husks and *tucumã* seeds (approximately 37%). The high oxygen amount in rice husks can be responsible for a higher volatile matter content (Sasmal *et al.*, 2012), but the lower calorific value. The calorific values were coffee husks (16.8 ± 0.1) MJ kg^{-1} ; rice husks (15.4 ± 0.1) MJ kg^{-1} and *tucumã* seeds (20.8 ± 0.1) MJ kg^{-1} . The biomasses studied have lower sulfur content ($< 1.0\%$), which implies a lower hydrogen sulfide gas production or SO_x emission during the gasification process (Sasmal *et al.*, 2012; Kumar *et al.*, 2009), enabling their use as feedstock for the bioenergy generation.

Rice husks have a higher ash content ($\approx 11\%$) in comparison to the other biomasses. According to Bin & Hongzhang (2010), a high ash content retards the enzymatic hydrolysis, *i.e.*, saccharification of biomass samples. Therefore, lignocellulosic material for the biofuel production demands washing for removal soluble water and adhered inorganic materials, with the customized pretreatment method occurs reduction in the ash content (Sasmal *et al.*, 2012; Folleto *et al.*, 2005).

The removal of moisture content from the biomasses started at around 70° C (water evaporation) and reached a maximum removal at around 105° C. Sasmal *et al.* (2012) showed that the removal of all moisture content present in the biomass fibers is very difficult due to the hydrophilic nature associated with the lignocellulosic materials; however, it was observed in this paper a small moisture quantity (around 8%).

Table 1. Moisture, ash content, elemental composition and high heat value of the samples *in natura*

Biomasses	Moisture (%)	Ash (%)	C (%)	H (%)	N (%)	S (%)	O (%)	HHV (MJ kg^{-1})
Coffee husks	8.2 ± 0.3	8.3 ± 2.8	43.13	5.93	1.55	0.67	32.22	16.79 ± 0.1
Rice husks	7.1 ± 0.4	11.2 ± 2.4	39.11	4.91	0.31	0.59	36.78	15.39 ± 0.1
<i>Tucumã</i> seeds	5.3 ± 0.3	5.3 ± 0.4	48.83	6.71	0.88	-	32.98	20.78 ± 0.1

Figures 1, 2 and 3 (a-c) show TG/DTG and DTA curves for the samples of coffee husks, rice husks, and *tucumã* seeds in 4 different atmospheres. The atmosphere of synthetic air in biomasses *in natura* was used to simulate a

Glauber Cruz, Carlos E. M. Braz, Sérgio L. Ferreira, Antonio M. dos Santos and Paula M. Crnkovic
 Physicochemical properties of brazilian biomasses: potential applications as renewable energy source

combustion process, pure nitrogen for pyrolysis and two concentrations of carbon dioxide and oxygen (60/80% CO₂ and 40/20% O₂) for oxy-fuel combustion.

The TG/DTG and DTA curves showed the thermal decomposition steps of the major constituent of lignocellulosic materials, *i.e.* hemicellulose, cellulose and lignin at their respective degradation temperatures (Yao *et al.*, 2008; Wu & Dollimore, 1998). In some biomasses the thermal decomposition of hemicellulose and cellulose occur at same stage (around 310 °C) and in this temperature a shoulder can be observed as overlapping peaks (Yao *et al.*, 2008).

TG/DTG thermograms (Figs. 1a and b) for the coffee husk samples showed that the samples had three thermal degradation steps in all the atmospheres (complex reactions mechanisms), but only two in inert atmosphere (without considering moisture loss steps).

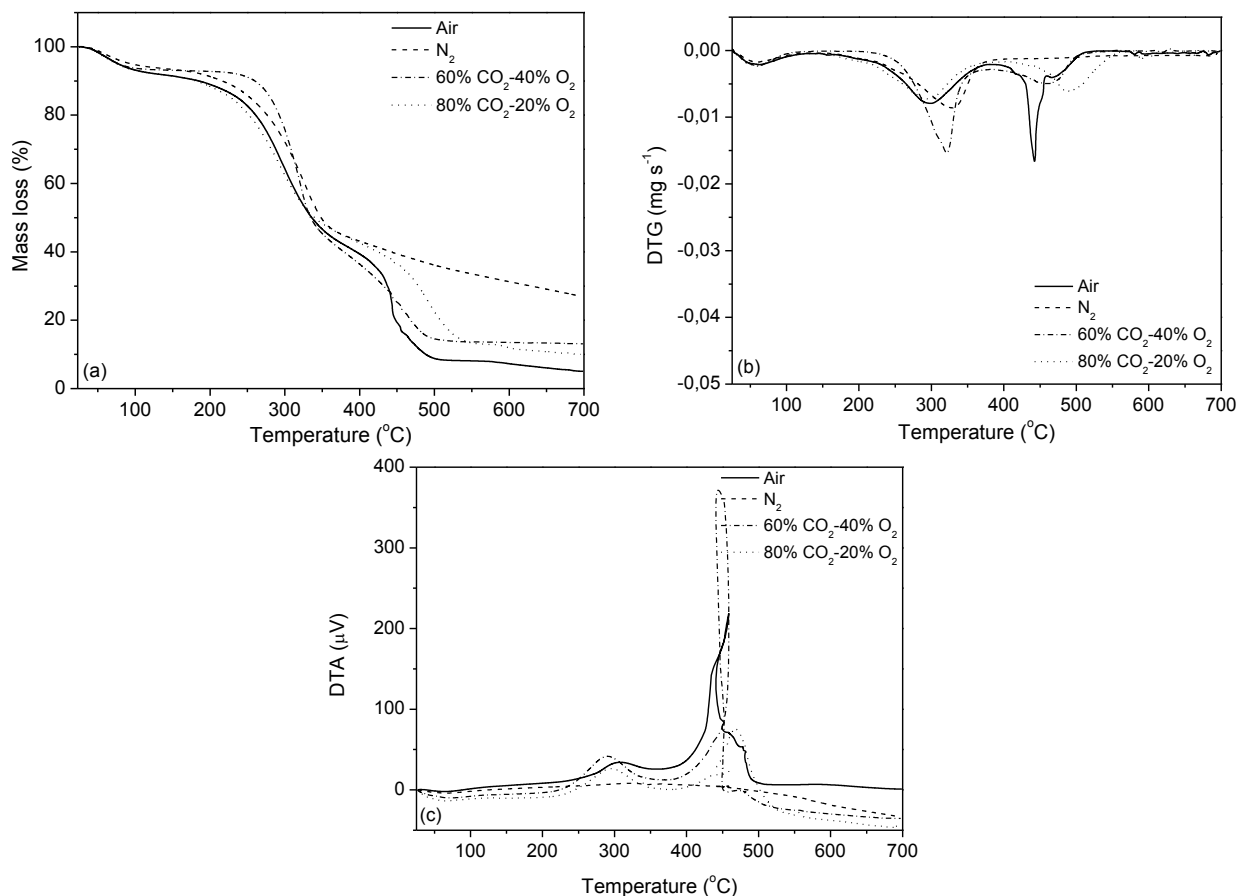


Figure 1. (a) TG, (b) DTG and (c) DTA curves of coffee husks in different atmospheres

The DTG curves (Fig. 1b) for the hemicellulose and cellulose decomposition showed that the degradation temperatures were the same in the combustion and oxy-fuel combustion (80% CO₂-20% O₂) atmospheres (approximately 295 °C). This can be explained by the gases concentration, indicating that a replace of CO₂ for N₂, has no effect significant in the combustion. The increase in oxygen concentration shifted the peaks to lower temperatures (Li *et al.*, 2009), whereas for samples under pyrolysis and oxy-fuel combustion (60% CO₂-40% O₂) atmospheres the peak temperatures were 328 and 320 °C, respectively.

The DTG curves for the coffee husks samples also showed that a higher mass loss was found for hemicellulose/cellulose (320 °C) and lignin (442 °C) decomposition in oxy-fuel combustion (60% CO₂-40% O₂) and synthetic air, respectively. According to Lai *et al.* (2011), the oxygen concentration strongly influences the volatile release and the combustion stage, benefiting ignition. The maximum temperature was around 490 °C in 80% CO₂-20% O₂ atmosphere.

The DTA curves (Fig. 1c) for the coffee husk samples showed only one endothermic peak related to the moisture loss (approximately 66 °C), and two exothermic peaks related to the thermal degradation of hemicellulose/cellulose (288-310 °C) and lignin (445-468 °C), respectively. Orsini *et al.* (2011) reported that the thermal decomposition of lignocellulosic materials occurs in energetic terms (endothermic or exothermic peaks), with consecutive and concomitant values.

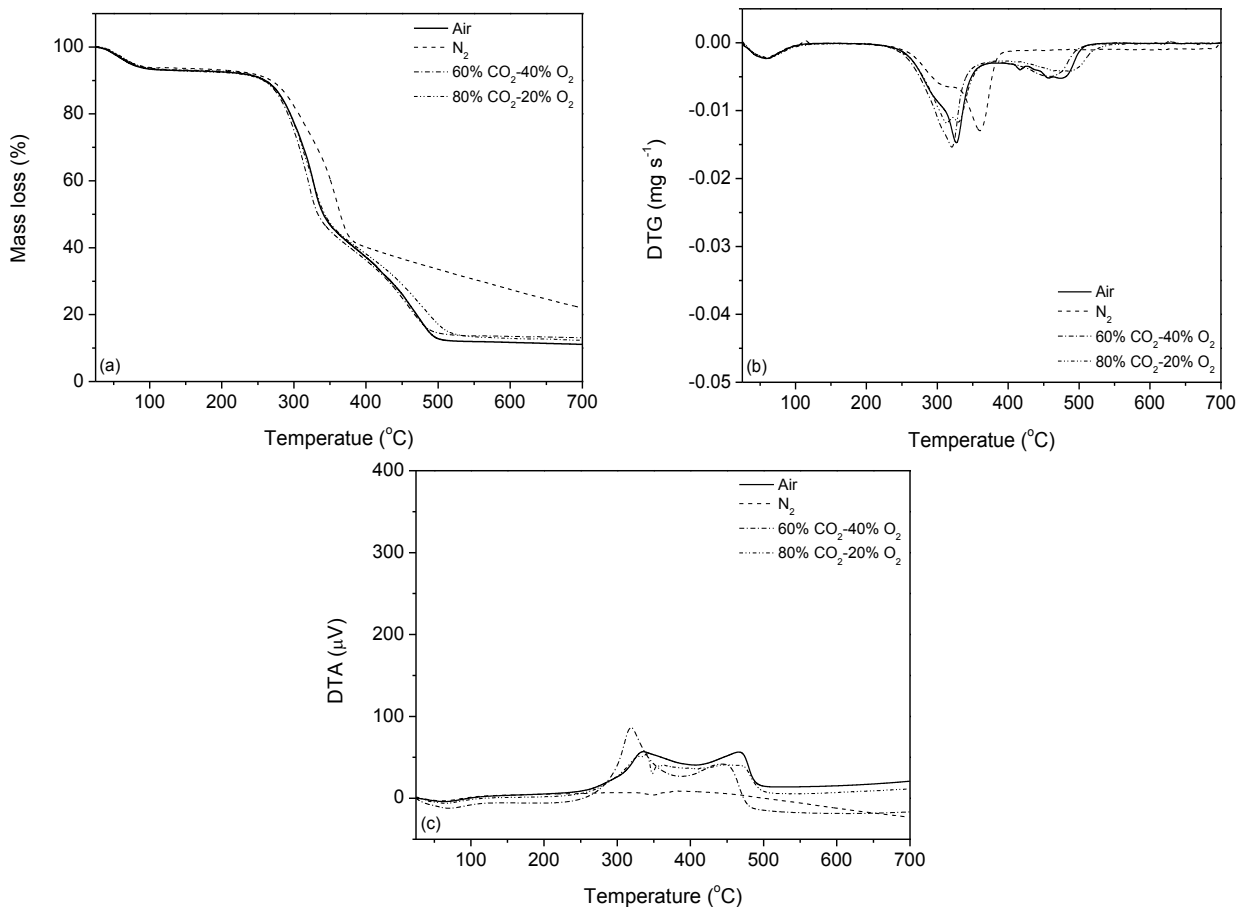


Figure 2. (a) TG, (b) DTG and (c) DTA curves of rice husks in different atmospheres

Figure 2a shows for rice husks that all the thermal decomposition steps of hemicellulose, cellulose and lignin in the different atmospheres. Only was observed some change in the pyrolysis ambient (temperature interval 150-420 °C), possibly due to the volatile releases (mainly CO₂, CO, H₂ and CH₄) and *biochar* formation (Markovska & Lyubchev, 2007).

The DTG curves (Fig. 2b) showed a peak and a "shoulder" at different temperatures for combustion and pyrolysis atmospheres. The temperatures of peak and shoulder for the combustion and pyrolysis were 310 and 327 °C, and 325 and 360 °C, respectively, whereas for two oxy-fuel combustion atmospheres were not observed the presence of "shoulders", and peak temperatures were around 320 °C. The temperatures ranged from 450 to 480 °C for all atmospheres in the lignin thermal degradation step.

Figure 2c (DTA curves) shows the endothermic and exothermic peaks at the determined temperatures. For all the atmospheres, an endothermic event of moisture loss is observed in approximately 62 °C. Large differences were observed in the pyrolysis atmosphere, with only one endothermic peak about 348 °C, whereas in other atmospheres, the thermal behavior was practically the same. For the combustion atmosphere were detected two exothermic peaks with the same intensity at 336 and 468 °C. The first peak corresponds to the thermal decomposition of hemicellulose and cellulose, and the second peak for lignin.

Furthermore, in oxy-fuel combustion atmosphere (60% CO₂-40% O₂) an exothermic peak more intense can be seen at 320 °C and other less intense at 447 °C. The peaks for oxy-fuel combustion atmosphere (80% CO₂-20% O₂) were at 336, 360 and 460 °C, which appear of the thermal decomposition of hemicellulose, cellulose, and lignin, respectively, confirming the peak displacement to lower temperatures by increasing of the oxygen concentration, due to formation a more oxidative ambient (Li *et al.*, 2009).

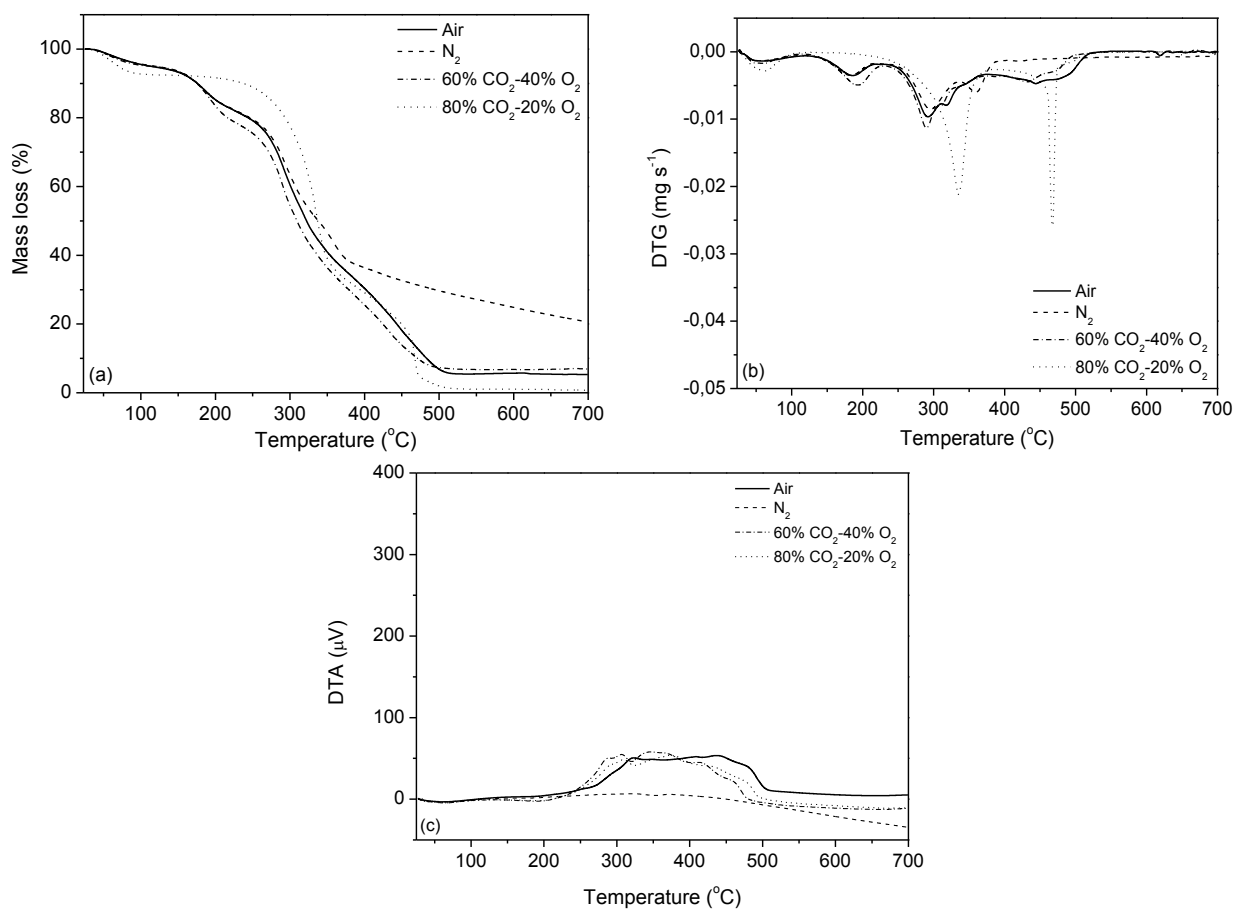


Figure 3. (a) TG, (b) DTG and (c) DTA curves of *tucumã* seeds in different atmospheres

Figure 3a shows the thermal degradation steps (TG curves) for *tucumã* seeds in the 4 atmospheres. As previously mentioned the curves exhibited the same thermal behavior.

From DTG curves (Fig. 3b) were observed three distinct decomposition steps of mass loss: hemicellulose (184-193 °C), cellulose (288-320 °C) and lignin (440-450 °C) for the combustion and oxy-fuel combustion (60% CO₂-40% O₂) atmospheres. The peak of decomposition of the lignin was displaced for 360 °C in the pyrolysis ambient, while two peaks were observed in the hemicellulose/cellulose (336 °C) and lignin decomposition (468 °C) for the oxy-fuel combustion atmosphere (80% CO₂-20% O₂).

Several exothermic peaks ranging from 250 to 500 °C were observed in the DTA curves for *tucumã* seed samples (Fig. 3c). The oilseed samples exhibited a highly exothermic behavior, which characterized oxidative decompositions during the thermal processes of combustion and oxy-fuel combustion (Santos *et al.*, 2012). Such a significant effect was not observed for the pyrolysis atmosphere, only an endothermic peak in 350 °C.

The ignition temperatures observed by TG curves for the coffee husk, rice husk and *tucumã* seed samples were 150, 250 and 270 °C, respectively. According to Li *et al.* (2009) and Lai *et al.* (2012), the ignition can be considered an initial process of the combustion phenomenon and an important key step in the stability and extinction of the flame and in the pollutants emissions.

Table 2. Average mass loss of biomasses for thermal decomposition processes

Atmospheres	Biomasses	Moisture (%)	Hemicellulose/cellulose (%)	Lignin (%)	Ashes (%)
synthetic air (combustion)	coffee husks	8.2 ± 0.3	73.7 ± 3.6	10.0 ± 1.1	8.3 ± 2.8
	rice husks	7.1 ± 0.4	53.3 ± 1.3	27.6 ± 0.3	11.2 ± 2.4
	<i>tucumã</i> seeds	5.3 ± 0.3	60.7 ± 0.7	28.9 ± 0.6	5.3 ± 0.4
nitrogen (pyrolysis)	coffee husks	6.3 ± 0.2	49.9 ± 0.4	16.7 ± 0.3	27.1 ± 0.6
	rice husks	6.2 ± 0.5	53.8 ± 0.5	17.5 ± 1.3	22.3 ± 2.1

	<i>tucumã</i> seeds	5.2 ± 0.1	54.2 ± 0.7	14.5 ± 0.1	20.8 ± 0.4
60% CO ₂ – 40% O ₂	coffee husks	7.6 ± 0.2	56.5 ± 1.5	25.1 ± 0.2	11.6 ± 0.8
	rice husks	6.7 ± 0.3	50.2 ± 0.9	27.3 ± 1.0	15.3 ± 0.8
	<i>tucumã</i> seeds	5.2 ± 0.3	50.3 ± 1.0	40.2 ± 2.3	5.2 ± 0.4
80% CO ₂ – 20% O ₂	coffee husks	8.2 ± 0.3	50.8 ± 1.9	29.9 ± 0.3	11.5 ± 0.7
	rice husks	7.1 ± 0.5	52.9 ± 0.9	24.1 ± 0.9	14.5 ± 0.8
	<i>tucumã</i> seeds	5.4 ± 0.3	54.8 ± 1.2	33.1 ± 1.0	5.3 ± 0.6

Table 2 summarizes the mass loss percentages in the samples *in natura* in the thermal degradation steps (moisture, hemicellulose, cellulose, lignin and ash content) by thermogravimetric analysis for the combustion, pyrolysis and oxy-fuel combustion processes. The wastes formed in the oxidizing atmosphere are called ashes, whereas in an inert atmosphere are denominated *biochar* (Babu, 2008; Lira *et al.*, 2013).

Table 2 shows a higher mass loss for the samples of coffee husks in combustion and oxy-fuel combustion (80% CO₂-20%O₂) atmosphere. About 8% of moisture and for hemicellulose/cellulose was 74% in combustion ambient. A high loss of lignin was obtained for the *tucumã* seed samples about 40% in oxy-fuel combustion (60% CO₂-20% O₂) atmosphere, and high ash content about 11% for rice husks.

3.2 X-Ray Diffractograms

Vandenbrink *et al.* (2012) reported that the Crystallinity Index (CI) of cellulosic biomass is an important factor for enhancing cellulose digestibility. CI is a measure of the fraction of crystalline cellulose for amorphous regions (lignin and hemicellulose) and inversely correlated with the enzymatic hydrolysis rate in microcrystalline cellulose. Samples with a high CI are believed to have a larger fraction of crystalline cellulose and are inefficiently hydrolyzed by cellulase (Vandenbrink *et al.*, 2012).

In order to compare the changes in the structural phases in the cellulose, the CIs of the samples *in natura* were calculated with reference to the peak diffraction intensities of the crystalline cellulose area (002) and amorphous regions (100) in plan by equation (1) (Vandenbrink *et al.*, 2012; Yu *et al.*, 2009; Yoshida *et al.*, 2008).

$$CI = \frac{(I_{002} - I_{am})}{I_{002}} \cdot 100, \quad (1)$$

where I_{002} is the intensity of the crystalline area of (002) plane at $2\theta = 22.5^\circ$ and I_{am} is the intensity of the amorphous region at $2\theta = 18.0^\circ$. I_{002} also means both crystalline and amorphous intensity (background) while I_{am} represents the only background intensity (Yu *et al.*, 2009).

Table 3. Crystallinity Index for samples *in natura*

Biomasses	Crystallinity Index (%)
Coffee husks	57.5 ± 0.7
Rice husks	64.3 ± 0.8
<i>Tucumã</i> seeds	57.4 ± 0.5

According to Zhang *et al.* (2008), the CI of the material surface is mainly related to the wax content (high molecular mass hydrocarbons and fatty acids) in the biomass. However, the overall crystallinity of the biomass depends on the wax and cellulose content and the nature of the bonds among cellulose, hemicellulose and lignin, forming a complex matrix (Guo & Catchmark, 2012; Naik *et al.*, 2010). Several researchers have reported that chemical, physical and thermal factors also affect the crystallinity of the biomass (Zhang *et al.*, 2008; Liu *et al.*, 2005).

Table 3 shows the maximum values of CI for the samples of rice husks, coffee husks and *tucumã* seeds. These values are indicative of large amorphous regions about 40% (hemicellulose and lignin together) in the samples, showing that rice husks can be more viable for enzymatic digestion and have more imperfect/amorphous hemicellulose in their composition than other two biomass materials (Yu *et al.*, 2009).

3.3 Fourier Transform Infrared Spectra

Figure 4(a-c) shows the spectroscopic behavior obtained in the infrared region for coffee husks, rice husks and *tucumã* seeds samples. According to Sasmal *et al.* (2012), the main characteristics in the FTIR spectra in biomass are attributed to the presence of different concentrations of hemicellulose, cellulose and lignin in the fibers.

Figure 4a shows the spectrum obtained for coffee husks *in natura* with the main bands presented in the following ranges: 3000, 2800, 1800 and 700 cm^{-1} . In a previous study, Reis *et al.* (2013) reported that bands at 2921 and 2847 cm^{-1} were attributed to the stretching of C-H bonds of methyl (-CH₃) group in the caffeine molecule, and successfully used to develop predictive models for a quantitative analysis of caffeine. Both bands show lower absorbance values in the spectra obtained for coffee husks, being the second band less evident in the coffee husk sample than in the coffee grain. Reis *et al.* (2013) also reported that other two bands at 2927-2925 and 2855 cm^{-1} are assigned to the asymmetric and symmetric stretchings of C-H in lipids. Such bands may be affected by caffeine and lipids levels. For coffee husks there are strong indications that these can be associated to the lipid concentrations.

It is evident that the spectrum of coffee husks *in natura* showed higher values of absorbance between 1700 and 1500 cm^{-1} . The bands in this range may be assigned to the axial deformation of C=C and C=N bonds in the aromatic ring of trigonelline (Reis *et al.*, 2013). The wave number from 1400 to 900 cm^{-1} is characterized by vibrations of several types of bonds, such as C-H, C-O, C-N and P-O. Chlorogenic acids, a family of esters formed between quinic acid and one to four residues of caffeic, *p*-coumaric and ferulic acids, that presents strong absorption in the region of 1450 and 1000 cm^{-1} . Carbohydrates also exhibit several absorption bands in the 1500 and 700 cm^{-1} region. Such a class of compounds is expected to substantially contribute to the observed bands. Particularly, the skeletal vibration modes of the glycosidic linkages in starch are observed in the wave numbers of 950 and 700 cm^{-1} (Reis *et al.*, 2013).

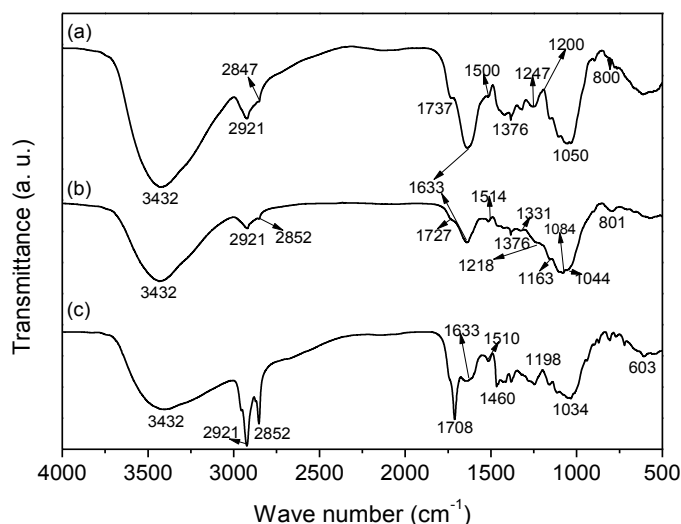


Figure 4. FTIR spectra: (a) coffee husks; (b) rice husks, and (c) *tucumã* seeds

According to Markovska & Lyubchev (2007), the absorption bands in the rice husks spectra are attributed to physically adsorbed water, functional groups of cellulose, hemicellulose and lignin, as well as the inorganic components in their composition (Fig. 4b). The wide and intense absorption band of maximum of approximately 3432 cm^{-1} can be attributed to their the valent vibrations of the O-H in water molecules with hydrogen bonds, or the OH groups present in cellulose, hemicellulose and lignin. The absorption bands at 1376, 1331, 1218 and 1044 cm^{-1} for rice husks can be related to the OH groups of lignin and polysaccharides, which form the husks structure. The band at 1633 cm^{-1} results from both the deformation vibrations of the water molecules (δ -H₂O) and the presence of C=C bonds in organic components. The more and less intense absorption bands at 2921 cm^{-1} and 2852 cm^{-1} are assigned to the asymmetric and symmetric of valent vibrations in C-H bonds in groups -CH₃ and -CH₂ for the structures of lignin, cellulose and hemicellulose. The band at 1727 cm^{-1} is related to the C=O bonds in aldehyde groups of hemicellulose, whereas the band at 1514 cm^{-1} is characteristic of the vibrations of the C=C bonds in the aromatic rings of lignin. The triplet in the 1000-1200 cm^{-1} region was considered from the superposition of vibrations of the C-OH and Si-O bonds in the siloxane groups. The intense band at 1050-1100 cm^{-1} (maximum at 1084 cm^{-1}) corresponds to valent vibrations of silicon-oxygen tetrahedrons (SiO₄). For the band at 1084 cm^{-1} it is also correct to affirm that main valent vibrations of the C-OH bond of cellulose are in the infrared region. A higher intensity at 1084 cm^{-1} is probably due to the superposition of the valent vibrations of the C-OH bond in the 1000-1200 cm^{-1} range and the valent vibrations of the Si-O bond. The presence of an absorption band at 780-790 cm^{-1} can be explained by symmetric valent vibrations of the Si-O bonds in the silicon-oxygen tetrahedrons (SiO₄) (Markovska & Lyubchev, 2007).

Figure 4c shows a band at 3432 cm^{-1} for *tucumã* seed, also attributed to either the valent vibrations of O-H in water molecules bonded by hydrogen bonds, or the OH groups present in cellulose, hemicellulose and lignin. The intense and

less intense absorption bands at 2921 cm^{-1} and 2852 cm^{-1} correspond to the asymmetric and symmetric valent vibrations of C–H bonds in function of $-\text{CH}_3$ (cellulose) and $-\text{CH}_2$ (cellulose) groups in the structures of lignin. A band ranges about 1200 cm^{-1} is characteristic of saturated esters (C–O–C), and in 1034 cm^{-1} is due to fatty acids. The spectroscopic profile results indicate that *tucumã* seeds exhibits a behavior of oilseeds in relation to the characteristic bands of fatty acids and saturated esters (Santos *et al.*, 2012).

3.4 Scanning Electron Microscopy

Figure 5 (a-c) shows the SEM micrographics for coffee husks, rice husks and *tucumã* seeds. The biomasses used in this study displayed different morphological characteristics.

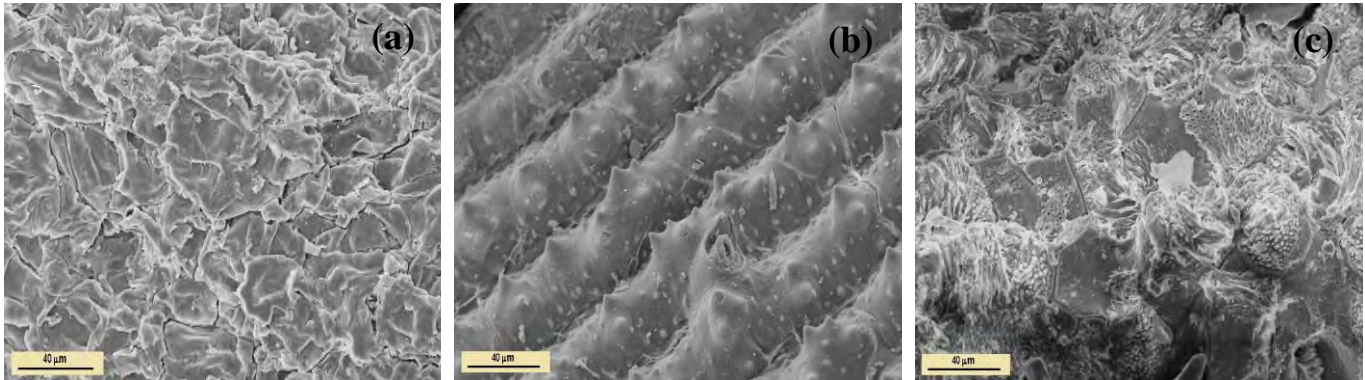


Figure 5. SEM micrographics: (a) coffee husk, (b) rice husk, and (c) *tucumã* seed samples

For coffee husks (Fig. 5a), the surface structure is well robust and contains large elongated grains without homogeneous surface, but the grain contour is well defined (Cruz *et al.*, 2012). In case of the Fig. 5b for rice husks has a well ordered and oriented morphology in format “parallel grooves” and external epidermis in its surface. There is a well defined separation and repetitions in the structure with linear profile, also is found blades format with “thorns” the coating (Uzunov *et al.*, 2012; Yu *et al.*, 2009). The *tucumã* seed samples (Fig. 5c) were characterized as a material very robust, dense, thicker wall, high density of pores in the surface. Moreover, the axial and radial structure of the pores also defines their geometric shape, which is attributed with to the “spongeous” characteristic material (highly porous) (Cruz *et al.*, 2012; Guimarães *et al.*, 2009).

3.5 Raman Scattering Spectroscopy

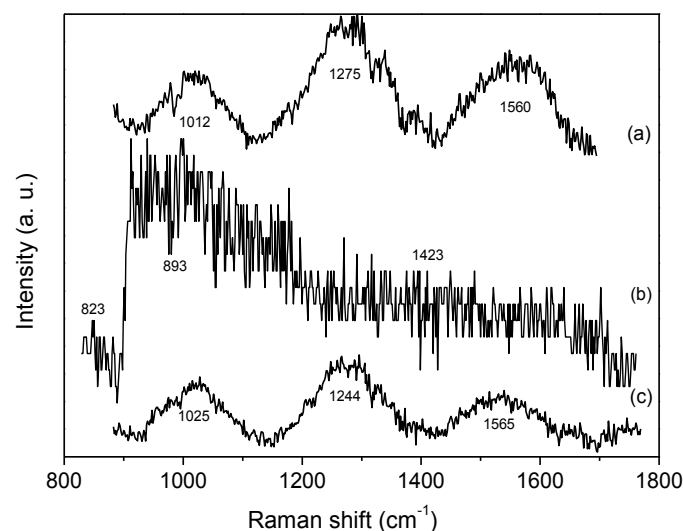


Figure 6. Raman spectra: (a) coffee husk, (b) rice husk, and (c) *tucumã* seed samples

According to Adapa *et al.* (2009), Raman spectroscopy has a good potential to determine the structural characteristics and the distribution of chemical components in lignocellulosic materials. The literature has reported that Raman spectroscopy can be successfully used to study lignocellulosic biomass in its chemical structure and spatial

distributions of cellulose, hemicellulose and lignin, and its application in various other wastes (food, feed, biocomposite, textile, paper and pulp industry) (Adapa *et al.*, 2009).

The use of Raman and Infrared Spectroscopy allows a complete view for both electrically symmetrical and non-symmetrical bonds. Raman effect depends on the polarity of the molecules. Assignment of the bands or wave numbers in the Raman spectra for lignocellulosic biomass is still in early stage. Adapa *et al.* (2009); Keown *et al.* (2008); Agarwal & Ralph (1997) reported that the band of macromolecules is oriented in the lignocellulosic fibers (sugarcane, black spruce and agricultural biomass materials) during FTIR-Raman analyzes.

Li *et al.* (2010) investigated by Raman the presence of aromatic skeletal lignin at 1510 cm^{-1} , syringyl and guaiacyl in condensed lignin at 1329 cm^{-1} for switch grass samples. Nanda *et al.* (2013) observed two main lignin features, which correspond to the aromatic ring stretch at 1595 cm^{-1} and ring-conjugated C=C bond at 1626 cm^{-1} (1650 cm^{-1} in case of pine wood). Furthermore, the band at 1056 cm^{-1} represent the C–O stretch in cellulose and hemicellulose and the band at 1375 cm^{-1} represent the deformation of the C–H bond. Keown *et al.* (2008) showed that the characteristic of broad peaks in Raman spectra for biomasses in the $1580\text{--}1610$ and $1325\text{--}1380\text{ cm}^{-1}$ ranges represents the G band (graphite) and D band (defect), which are common in biochars structures.

Figure 6 (a-c) shows the Raman spectra of the biomass samples *in natura* (first order spectra). According to Agarwal & Ralph (1997) and Nanda *et al.* (2013), the major vibrations in the Raman spectra of biomasses were found in the $1595\text{--}1650\text{ cm}^{-1}$ regions due to the lignin presence, whereas cellulosic and hemicellulosic components are present in the $973\text{--}1183\text{ cm}^{-1}$ range. For coffee husks and *tucumã* seeds (Figs. 6a and c) presents three large bands with the (1012 , 1275 , and 1560 cm^{-1}) and (1025 , 1244 and 1565 cm^{-1}) intensity, which signified a high concentration of hemicellulose, cellulose and lignin. The presence of a higher lignin concentration can be showed by bands intensity of rice husks (Fig. 6b) at 823 cm^{-1} , 893 cm^{-1} and 1423 cm^{-1} . At 900 cm^{-1} peak is reflective to amorphous cellulose, whereas at 1098 cm^{-1} is assigned to crystalline cellulose (Nanda *et al.*, 2013; Sasmal *et al.*, 2012).

3.6 Wettability or Contact Angle

According to Azevedo *et al.* (2009), the wettability measure is a simple and easy method that provides information about the crystallographic structure of the surface. It is also correlated with chemical nature and functional groups associated to their variations in contact with different liquid types. This technique has been largely used for the characterization of carbonaceous materials (micro and nanodiamond, boron doped diamond, carbon nanotubes and others) (Ostrovskaya *et al.*, 2007; Zhou *et al.*, 2006; Kaibara *et al.*, 2003; Pinzari *et al.*, 2001).

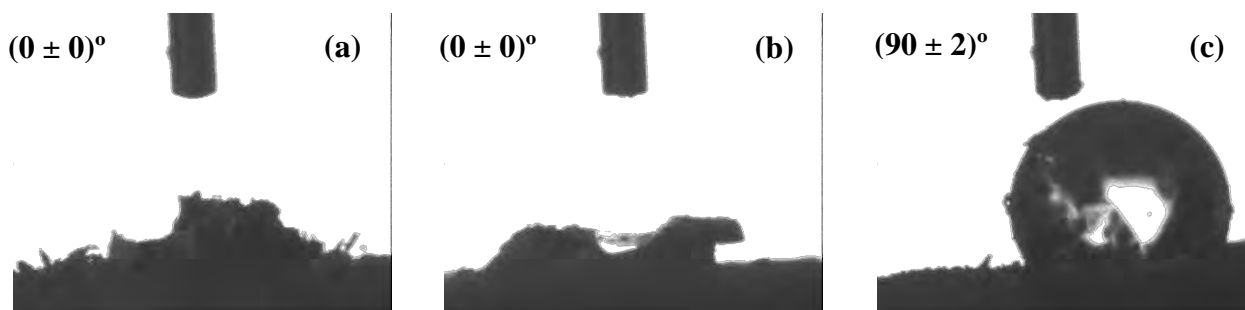


Figure 7. Contact angles: (a) coffee husk, (b) rice husk, and (c) *tucumã* seed samples

This technique was employed in this study as a new technology (nanotechnology and biotechnology) to evaluate surface properties of lignocellulosic materials through the functional groups (carboxyl and carbonyl) and terminations (hydrogenated and oxygenated).

Figure 7 (a-c) shows the Contact angles for coffee husks, rice husks and *tucumã* seeds *in natura*. According to Sasmal *et al.* (2012), lignocellulosic materials have mainly a hydrophilic character ($\theta < 90^\circ$), although lignin shows hydrophobic character ($\theta > 90^\circ$) (Wiman *et al.*, 2012). These values of CA, possibly also can be related to rough and porous surfaces or terminations with oxygen in their surface (carbonyl or carboxyl) (Uzunov *et al.*, 2012; Azevedo *et al.*, 2009). Can be observed for coffee and rice husks samples (Fig. 7a and b, respectively), that the water drop perfectly wets to the biomass surface (by spreading). For the *tucumã* seed samples (Fig. 7c), the effect of wettability was fully opposite the two previous samples, which presented hydrophobic character, possibly due to its oleophilic natural character (Uzunov *et al.*, 2012) and by the presence of waxy or oily substances in their surface or composition. This can contribute to an ineffective fiber-matrix bond and a poorly wetted surface (Santos *et al.*, 2012; Vilay *et al.*, 2008).

4. CONCLUSIONS

The physicochemical characterization of the three biomasses *in natura* indicated that the *tucumã* seed samples are more favorable for the bioenergy production, as they showed a high calorific value (approximately 21 MJ kg^{-1}) and a

high sugar concentration (hemicellulose/cellulose, average 60%) than lignin (29%), in addition low content of moisture (5.3%) and ashes (5.3%).

The thermal degradation steps of the main lignocellulosic constituent of the biomasses in combustion, pyrolysis and two oxy-fuel combustion atmospheres were identified by Thermal Analysis (TG/DTG and DTA), which presented semi-quantitative amounts of hemicellulose, cellulose and lignin, and the presence of endothermic and exothermic events during the main thermal conversion processes. The ignition temperatures were 150, 250 and 270 °C for coffee husk, rice husk and *tucumã* seed samples, respectively.

O-containing functional groups in lignocellulosic materials were identified by FTIR analysis, but has restricted application in the exploring the less-polar aromatic structures, while X-Ray and Raman were used to evaluate structural features of such material, because it is sensitive for both crystalline and amorphous constructions. Wettability showed that coffee and rice husk samples showed a superhydrophilic character ($\theta=0^\circ$), while *tucumã* seed samples presented a hydrophobic character ($\theta>90^\circ$).

The present study has showed that the three brasilian biomass can be utilized as feedstock for the biofuel or bioenergy production, independent of the conversion process, such as enzymatic hydrolysis, gasification or fermentation to ensure the demand of the second generation biofuel.

5. ACKNOWLEDGEMENTS

The authors gratefully acknowledge CAPES (DS00011/07-0), CNPq, and FAPESP (2012/00639-2) for the financial support, Thermal Engineering and Fluids Laboratory (NETeF) at University of São Paulo (USP), and Dr^a. Adriana Faria de Azevedo (National Institute for Space Research - INPE) for the Raman and Wettability measurements.

6. REFERENCES

- Adapa, P., Karunakaran, C., Tabil, L., Schoenau, G. (2009) Potencial applications of Infrared and Raman spectromicroscopy for agricultural biomass. *J. Agric. Eng. Int.* 11 (2009) 1081-1096.
- Agarwal, U.P., Ralph, S.A. (1997) FT-Raman spectroscopy of wood: identifying contributions of lignin and carbohydrate polymers in the spectrum of black spruce (*Picea mariana*). *App. Spectrosc.* 51 (1997) 1648-1655.
- Aghamohammadi, N., Sulaiman, N.M.N., Aroua, M.K. (2011) Combustion characteristics of biomass in South East Asia. *Biomass & Bioenergy.* 35 (2011) 3884-3890.
- Álvarez, L., Gharebaghi, M., Pourkashanian, M., Williams, A., Riaza, J., Pevida, C., Pis, J.J., Rubiera, F. CFD modeling of oxy-coal combustion in a entrained flow reactor. *Fuel Proces. Technol.* 92 (2011) 1489-1497.
- Arias, B., Pevida, C., Rubiera, F., Pis, J.J. (2008) Effect of biomass blending on coal ignition and burnout during oxy-fuel combustion. *Fuel.* 87 (2008) 2753-2579.
- Azevedo, A.F., Matsushima, J.T., Vicentin, F.C., Baldan, M.R., Ferreira, N.G. (2009) Surface characterization of NCD films as a function of sp²/sp³ carbon and oxygen conten. *Appl. Surf. Sci.* 255 (2009) 6565-6570.
- Babu, B.V. (2008) Biomass pyrolysis: a state-of-the-art review. *Biof. Bioprod. Bioref.* 2 (2008) 393-414.
- Bin, Y., Hongzhang, C. (2010) Effect of the ash on enzymatic hydrolysis of setam-exploded rice straw. *Bioresour. Technol.* 101 (2010) 9114-9119.
- Cruz, G., Ávila, I., dos Santos, A.M., Crnkovic, P.M. (2012) "Evaluation of the thermal properties and morphological of biomass *in natura*" (in portuguese) Proceedings of the 7th National Congress of Mechanical Engineering - CONEM2012, São Luís, Brazil, 9pp.
- Folletto, E.L., Hoffmann, R., Hoffmann, R.S., Portugal Jr, U.L., Jahn, S.L. (2005) Applicability of rice husk ash (in portuguese). *Quim. Nova.* 28 (2005) 1055-1060.
- García, R., Pizarro, C., Lavín, A.G., Bueno, J.L. (2010) Characterization of Spain biomass wastes for energy use. *Bioresour. Technol.* 103 (2012) 249-258.
- Guimarães, J.L., Frollini, E., da Silva, C.G., Wypych, F., Satyanarayana, K.G. (2009) Characterization of banana, sugarcane bagasse and sponge gourd fibers of Brazil. *Indust. Crops Prod.* 30 (2009) 407-415.
- Guo, J., Catchmark, J.M. (2012) Surface area and porosity of acid hydrolyzed cellulose nanowhiskers and cellulose produced by *Gluconacetobacter xylinus*. *Carbohydr. Polym.* 87 (2012) 1026-1037.
- Han, J., Kim, H. (2008) The reduction and control technology of tar during biomass gasification/pyrolysis: an overview. *Renew. Sust. Energy Rev.* 12 (2008) 397-416.

- Kaibara, Y., Sugata, K., Tachiki, M., Umezawa, H., Kawarada, H. (2003) Control wettability of the hydrogen-terminated diamond surface and the oxidized diamond surface using an atomic force microscope. *Diam. Relat. Mater.* 12 (2003) 560-564.
- Keown, D.M., Li, X., Hayashi, J.I., Li, C.Z. (2008) Evolution of biomass char structure during oxidation in O₂ as revealed with FT-Raman spectroscopy. *Fuel Process. Technol.* 89 (2008) 1429-1435.
- Kumar, A., Jones, D., Hanna, M. (2009) Thermochemical biomass gasification: a review of the current status of the technology. *Energies.* 2 (2009) 556-581.
- Krüss Information Database: Installation and Operation V1-02 (2005). *Equipment Handbook*, 167 pp.
- Lai, Z.H., Ma, X.Q., Tang, Y.T., Lin, H. (2011) A study on municipal solid waste (MSW) combustion in N₂/O₂ and CO₂/O₂ atmosphere from the perspective of TGA. *Energy.* 36 (2011) 819-824.
- Lai, Z.H., Ma, X.Q., Tang, Y.T., Lin, H., Chen, Y. (2012) Thermogravimetry analyses of combustion of lignocellulosic materials in N₂/O₂ and CO₂/O₂ atmospheres. *Bioresour. Technol.* 107 (2012) 444-450.
- Leroy, V., Cancellieri, D., Leoni, E. (2006) Chemical and thermal analysis of ligno-cellulosic fuels. *Forest Ecol. Manag.* 234S (2006) S125.
- Li, C., Knierim, B., Manisseri, C., Arora, R., Scheller, H. V., Auer, M., Vogel, K. P., Simmons, B. A., Singh, S. (2010) Comparison of dilute acid and ionic liquid pretreatment of switchgrass: Biomass recalcitrance, delignification and enzymatic saccharification. *Bioresour. Technol.* 101 (2010) 4900-4906.
- Li, Q., Zhao, C., Chen, X., Wu, W., Li, Y. Comparison of pulverized coal combustion in air and in O₂/CO₂ mixtures by thermo-gravimetric analysis. *J. Anal. Appl. Pyrol.* 85 (2009) 521-528.
- Lira, C.S., Berruti, F.M., Palmisano, P., Berruti, F., Briens, C., Pécora, A.A.B. (2013) Fast pyrolysis of *Amazon tucumã* (*Astrocaryum auleatum*) seeds in a bubbling fluidized bed reactor. *J. Anal. Appl. Pyrol.* 99 (2013) 23-31.
- Liu, R.G., Yu, H., Huang, Y. (2005) Structure and morphology of cellulose in wheat straw. *Cellulose.* 12 (2005) 25-34.
- Markovska, I.G., Lyubchev, L.A. (2007) A study on the thermal destruction of rice husk in air and nitrogen atmosphere. *J. Therm. Anal. Cal.* 89 (2007) 809-814.
- Naik, S., Goud, V.V., Rout, P.K., Jacobson, K., Dalai, A.K. (2010) Characterization of Canadian biomass for alternative renewable biofuel. *Renew. Energ.* 35 (2010) 1624-1631.
- Nanda, S., Mohanty, P., Pant, K.K., Naik, S., Kozinski, J.A., Dalai, A.K. (2013) Characterization of North American lignocellulosic biomass and biochars in terms of their candidacy for alternate renewable fuels. *Bioenerg. Res.* 6 (2013) 663-677.
- Orsini, R.R., Filho, E.M., Mercuri, L.P., Matos, J.R., de Carvalho, F.M.S. (2011) Thermoanalytical study of inner and outer residue of coffee harvest. *J. Therm. Anal. Calorim.* 106 (2011) 741-745.
- Ostrovskaya, L., Perevertailo, V., Ralchenko, V., Saveliev, A., Zhuravlev, V. (2007) Wettability of nanocrystalline diamond films. *Diam. Relat. Mater.* 16 (2007) 2109-2113.
- Pinzari, F., Ascarelli, P., Cappelli, E., Mattei, G., Giorgi, R. (2001) Wettability of HF-CVD diamond films. *Diam. Relat. Mater.* 10 (2001) 781-785.
- Ramajo-Escalera, B., Espina, A., García, J.R., Sosa-Arno, J.H., Nebra, S.A. (2006) Model-free Kinetics applied to sugarcane bagasse combustion. *Thermochim. Acta.* 448 (2006) 111-116.
- Reis, N., Franca, A.S., Oliveira, L.S. Discrimination between roasted coffee, roasted corn and coffee husks by Diffuse Reflectance Infrared Fourier Transform Spectroscopy. *Food Sci. Technol.-LWT.* 50 (2013) 715-722.
- Riaza, J., Álvarez, L., Gil, M.V., Pevida, C., Pis, J.J., Rubiera, F. (2011) Effect of oxy-fuel combustion with steam addition on coal ignition and burnout in an entrained flow reactor. *Energy* 36 (2011) 5314-5319.
- Santos, O.V., Corrêa, N.C.F., Soares, F.A.S.M., Gioielli, L.A., Costa, C.E.F., Lannes, S.C.S. (2012) Chemical evaluation and thermal behavior of Brazil nut oil obtained by different extraction process. *Food Res. Int.* 47 (2012) 253-258.
- Sasmal, S., Goud, V.V., Mohanty, K. (2012) Characterization of biomasses available in the region of North-East India for production of biofuels. *Biomass & Bioenergy* 45 (2012) 212-220.
- Senneca, O. (2007) Kinetics of pyrolysis, combustion and gasification of three biomass fuels. *Fuel Process. Technol.* 88 (2007) 87-97.
- Tsai, W.T., Lee, M.K., Chang, Y.M. (2006) Fast pyrolysis of rice straw, sugarcane bagasse and coconut shell in a inductor-heating reactor. *J. Anal. Appl. Pyrol.* 76 (2006) 230-237.

Proceedings of the 22nd International Congress of Mechanical Engineering – COBEM2013
November 3-7, 2013, Ribeirão Preto, SP, Brazil

- Uzunov, I., Uzunova, S., Angelova, D., Gigova, A. (2012) Effects of the pyrolysis process on the oil sorption capacity of rice husk. *J. Anal. Appl. Pyrol.* 98 (2012) 166-176.
- Van der Stelt, M.J.C., Gerhauser, H., Kiel, J.H.A., Ptasinski, K.J. (2011) Biomass upgrading by torrefaction for the production of biofuels: A review. *Biomass & Bioenergy.* 35 (2011) 3748-3762.
- Vandenbrink, J.P., Hilten, R.N., Das, K.C., Paterson, A.H., Feltus, F.A. (2012) Analysis of crystallinity index and hydrolysis rates in the bioenergy *Sorghum bicolor*. *Bioenerg. Res.* 5 (2012) 387-397.
- Vilay, V., Mariatti, M., Taib, R.M., Todo, M. (2008) Effect of fiber surface treatment and fiber loading on the properties of bagasse fiber-reinforced unsaturated polyester composites. *Compos. Sci. Technol.* 68 (2008) 631-638.
- Yao, F., Wu, Q., Lei, Y., Guo, W., Xu, Y. (2008) Thermal decomposition kinetics of natural fibers: Activation energy with dynamic thermogravimetric analysis. *Polym. Degrad. Stabil.* 93 (2008) 90-98.
- Yoshida, M., Liu, Y., Uchida, S., Kawarada, K., Ukagami, Y., Ichinose, H., Kaneko, S., Fukuda, K. (2008) Effects of cellulose crystallinity, hemicellulose, and lignin on the enzymatic hydrolysis of *Miscanthus sinensis* to monosaccharides. *Biosci. Biotechnol. Biochem.* 72 (2008) 805-810.
- Yu, C.T., Chen, W.H., Men, L.C., Hwang, W.S. (2009) Microscopic structure features changes of rice straw treated by boiled acid solution. *Ind. Crop. Prod.* 29 (2009) 308-315.
- Wiman, M., Dienes, D., Hansen, M.A.T., van der Meulen, T., Zacchi, G., Lidén, G. (2012) Cellulose accessibility determines the rate of enzymatic hydrolysis of steam-pretreated spruce. *Bioresour. Technol.* 126 (2012) 208-215.
- Wu, Y., Dollimore, D. (1998) Kinetic studies of thermal degradation of natural cellulose materials. *Thermochim. Acta.* 324 (1998) 49-57.
- Zhang, L.H.; Dong, L., Wang, L.J., Wang, T.P., Zhang, L., Chen, X.D. (2008) Effect of steam-explosion on biodegradation of lignin in wheat straw. *Bioresour. Technol.* 97 (2008) 661-665.
- Zhao, W., Li, Z., Wang, D., Zhu, Q., Sun, R., Meng, B., Zhao, G. (2008) Combustion characteristics of different parts of corn straw and NO formation in a fixed bed. *Bioresour. Technol.* 99 (2008) 2956-2963.
- Zhou, Y., Wang, B., Song, X., Li, E., Li, G., Zhao, S., Yan, H. (2006) Control over the wettability of amorphous carbon films in a large range from hydrophilicity to super-hydrophobicity. *Appl. Surf. Sci.* 253 (2006) 2690-2694.

7. RESPONSIBILITY NOTICE

The authors are the only responsible for the printed material included in this paper.